THE PUBLISHING HOUSE
OF THE ROMANIAN ACADEMY

PROCEEDINGS OF THE ROMANIAN ACADEMY, Series A,
Volume 18, Number 4/2017, pp. 370–377

COMPLEX DYNAMICS IN HYSTERETIC NONLINEAR OSCILLATOR CIRCUIT

Carmen GRIGORAS [1,2], Victor GRIGORAS [3]

[1] „Gr.T. Popa" University of Medicine and Pharmacy of Iaşi, 700115, Romania
[2] Institute of Computer Science of the Romanian Academy, Iaşi, 700481, Romania
[3] „Gheorghe Asachi" Technical University of Iaşi, 700506, Romania
Corresponding author: Victor GRIGORAS, E-mail: grigoras@etti.tuiasi.ro

Abstract. The present paper introduces a new, fourth order, analogue chaos generator, aiming at noise, random pulse and spread spectrum signal applications. The proposed system has a simpler implementation compared to other circuits reported in the literature, using only one nonlinear element, namely a Schmitt trigger type hysteretic block, and leading to a uniform circuit structure. The analysis of the system dynamics shows richer behavior than previously reported ones, including two single scroll and one double scroll strange attractors, as well as several limit cycles with period multiplicity, obtained for different ranges of coefficients values. Furthermore, we designed and measured the circuit implementation of our system, obtaining results in good accordance with the theoretical and simulation results.

Key words: bifurcation, chaos, noise generators, nonlinear circuits, nonlinear dynamical systems.

1. INTRODUCTION

The present paper introduces a new hysteretic nonlinear system, exhibiting rich dynamics, including periodic and chaotic oscillations. The aim of our research is to develop a chaotic generator implementable with simple electronic circuit, based on uniform, i.e. similar topology building blocks, applicable in a wide range of domains where noise and random pulses are needed.

There are many classic analog chaotic generators reported in the literature, some of them implementable using electronic circuits. Some of the first reported chaotic generators use multipliers as nonlinear functions. Single multiplier nonlinear systems include the Rossler chaotic system [1]. Examples of two multipliers nonlinear systems exhibiting chaotic dynamics include the Lorenz system [2] and the Chen attractor [3]. Such nonlinear systems would lead to non-uniform electronic implementations, based on operational amplifiers (OA) and analog multipliers structures, which are difficult to integrate and compensate for device non-idealities, as highlighted in [4]. Research was conducted to simplify the implementation of such complex behavior nonlinear systems, by using only the sign of one of the state variables [5], but that did not eliminate the need for analog multipliers. A chaotic system designed starting from a circuit implementation is Chua's oscillator [6], which uses switching diodes in its nonlinearity, but uses also an inductance, that poses integration difficulties. In depth studies were made on hysteretic systems exhibiting complex dynamic properties [7, 8]. These systems suffer too from non-uniform topology, involving the use of semiconductor diodes as switching elements, which require higher currents, leading to lower and less controllable switching speed. Other simple chaos generators have also been proposed [9, 10], yielding only one chaotic attractor, based on piecewise linear algebraic nonlinearities, implemented with semiconductor diodes as switching elements, with the aforementioned drawbacks. Complex nonlinear dynamics were highlighted in [11, 12] for circuits with a piezoelectric selective element that increase complexity and reduces the possibility to integrate the generator on a single chip.

The system proposed in our paper is a fourth order analog nonlinear circuit, using a Schmitt trigger hysteretic nonlinearity, leading to simple, uniformly implemented only with operational amplifiers resistor and capacitor components. Compared to previously reported systems, the present proposal yields far more complex dynamics, with different types of behavior, for different ranges of parameter values. Both simulations and

measurements performed on the circuit showed the presence of a double scroll and two single scroll strange attractors, as well as limit cycles with different period multiplicity. The complexity of the circuit dynamic and statistic properties confirm the desired possibility of application for noise, spread spectrum clock signals and random pulse generation.

The following section of this paper presents the design and dynamic analysis of the proposed system, including relevant simulation results. The third section concentrates on circuit design and implementation, with measurement results confirming the desired system properties. The concluding section highlights the advantages of the proposed circuit and its possible applications.

2. SYSTEM DYNAMICS ANALYSIS

We propose a nonlinear system architecture based on a previously reported system [13], which was described by the state equations:

$$\begin{cases} \mathrm{d}x/\mathrm{d}t = a \cdot y - z \\ \mathrm{d}y/\mathrm{d}t = -a \cdot x + z \\ \mathrm{d}z/\mathrm{d}t = -x - y - a \cdot z + \mathrm{sign}(x) \end{cases} . \tag{1}$$

In order to obtain richer dynamics, we increase the order of the system (1), replacing the comparator type nonlinearity, sign(x), with an extra state variable, *v(t)*, given by a hysteretic element, with relay characteristic, described by the state equation (2), deduced in Appendix A:

$$\begin{cases} \mathrm{d}v/\mathrm{d}t = -\dfrac{v}{\tau} + \mathrm{Th} \cdot \dfrac{G}{\tau} \cdot \mathrm{sat}(v) - \dfrac{G}{\tau} \cdot u \\ w = \mathrm{sat}(v) \end{cases} . \tag{2}$$

In (2), v denotes the supplementary state variable, u and w the input and output of the Schmitt trigger, G is the open loop gain and τ the time constant of the OA in the Schmitt trigger circuit and *Th* the positive switching threshold scale factor of the Schmitt trigger. The nonlinear function, *sat*(v), in equation (2), is a normalized piecewise linear model of the saturation characteristic of the OA, (3):

$$\mathrm{sat}(v) = \begin{cases} -1 \text{ if } v < -1 \\ v \text{ if } |v| < 1 \\ 1 \text{ if } v > 1 \end{cases} . \tag{3}$$

The resulting nonlinear input-output characteristic of the Schmitt trigger, presented in Fig. 1, shows the behavior of the nonlinear dynamic element.

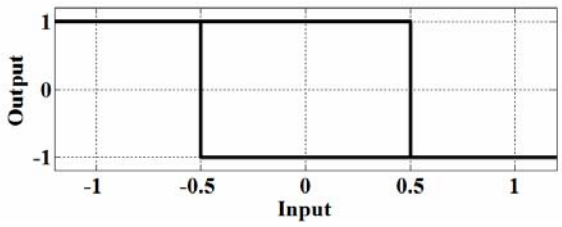

Fig. 1 – Inverting type Schmitt trigger hysteretic characteristic for Th = 0.5.

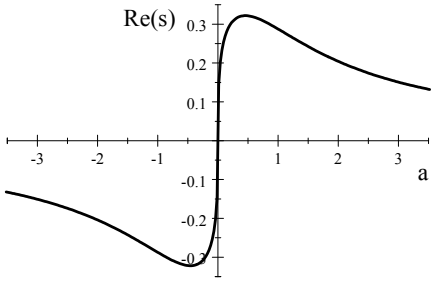

Fig. 2 – The plot of the real part of the complex Jacobian eigenvalues, at the variation of the *a* coefficient.

By making the aforementioned modifications to the initial system (1), with the hysteretic model (2), the state equations for the proposed fourth order nonlinear system result in the form:

$$\begin{cases} \mathrm{d}x/\mathrm{d}t = a \cdot y - z \\ \mathrm{d}y/\mathrm{d}t = -a \cdot x + z \\ \mathrm{d}z/\mathrm{d}t = -x - y - a \cdot z + \mathrm{sat}(v) \\ \mathrm{d}v/\mathrm{d}t = -G/\tau \cdot (-x) - v/\tau + \mathrm{Th} \cdot G/\tau \cdot \mathrm{sat}(v) \end{cases}. \tag{4}$$

We start the dynamic analysis of the system (4) with the calculation of its equilibrium points by solving the algebraic system:

$$\begin{cases} a \cdot y - z = 0 \\ -a \cdot x + z = 0 \\ -x - y - a \cdot z \pm 1 = 0 \\ G/\tau \cdot x - v/\tau \pm \mathrm{Th} \cdot G/\tau = 0 \end{cases}. \tag{5}$$

Notably, any equilibrium point for which $|v| < 1$ cannot be attained, because the Schmitt trigger will never settle in this range of values. The sign of the last terms in the last two equations in (5) is '+' if the Schmitt trigger is in the high state and '–' in the opposite case. With the same sign convention as before, the solutions of the system (5) are given by:

$$x = y = \pm\frac{1}{a^2+2}; \quad z = \pm\frac{a}{a^2+2}; \quad v = \pm G\left(\mathrm{Th} + \frac{1}{a^2+2}\right). \tag{6}$$

In both cases present in (6), the Jacobian of the system is independent of the state variables values:

$$J(\mathbf{x}) = \begin{bmatrix} 0 & a & -1 & 0 \\ -a & 0 & 1 & 0 \\ -1 & -1 & -a & 0 \\ G/\tau & 0 & 0 & -1/\tau \end{bmatrix}. \tag{7}$$

Thus, both equilibriums will be simultaneously stable or unstable. The eigenvalues of the Jacobian $J(\mathbf{x})$ (7) can be found by symbolic calculation, as:

$$s_1 = -\frac{1}{\tau};\ s_2 = -\frac{a}{3} + 2\rho;\ s_{3,4} = -\frac{a}{3} - \rho \pm j\frac{\sqrt{3}}{2}\rho;\ \rho = \frac{\sigma}{2} - \frac{1/9 \cdot a^2}{\sigma};\ \sigma = \sqrt[3]{\frac{10a^3}{27} - a + \sqrt{\frac{4a^6}{27} - \frac{20a^4}{27} + a^2}}. \tag{8}$$

From the plot in Fig. 2, we see that, for positive values of the coefficient a, the real part of the Jacobian complex eigenvalues, $s_{3,4}$ in (8), are positive, leading to the conclusion that both equilibrium points are unstable.

The dissipative character of the system can also be verified analytically, by calculating the divergence of the vector field (4):

$$\nabla\mathbf{f}(\mathbf{x}) = \frac{\partial f_1(\mathbf{x})}{\partial x} + \frac{\partial f_2(\mathbf{x})}{\partial y} + \frac{\partial f_3(\mathbf{x})}{\partial z} + \frac{\partial f_4(\mathbf{x})}{\partial v} = \begin{cases} -a - \dfrac{1}{\tau} + \mathrm{Th} \cdot G/\tau & \Leftrightarrow \quad |v| < 1 \\ -a - \dfrac{1}{\tau} & \Leftrightarrow \quad |v| \geq 1 \end{cases}. \tag{9}$$

Due to the fact that the Schmitt trigger settles only at one of the stable states $\mathrm{sat}(v) = +/- 1$, only the second alternative in equation (9) is observable, leading to:

$$\nabla\mathbf{f}(\mathbf{x}) = -a - \frac{1}{\tau}. \tag{10}$$

For all positive values of the coefficients a and τ, the divergence of the vector field (10) is negative, confirming the system's dissipative nature. The ergodic and sensitive properties of the analyzed system cannot be verified analytically and will be estimated by simulation.

In order to choose the equations coefficients, for the desired system behavior, we performed in depth parametric analysis, to determine the nonlinear dynamics of the hysteretic system, for different values of the Th threshold scaling factor and *a* parameter. By symmetrically varying the Schmitt trigger switching thresholds factors, Th, we obtained bifurcation diagrams, similar to the one presented in Fig. 3 for $a = 2.21$, highlighting chaotic behavior for most parameter values, with short periodic interruptions. For different values of the Th threshold factor, bifurcation diagrams at the variation of the parameter *a* show alternating periodic and chaotic regions, as shown in the example depicted in Fig. 4, for the value of Th = 0.022. Three dimensional representations of the results of the parametric analysis were avoided, because the wide regions of chaos would hide the short periodic interruptions present in the 2-D representations.

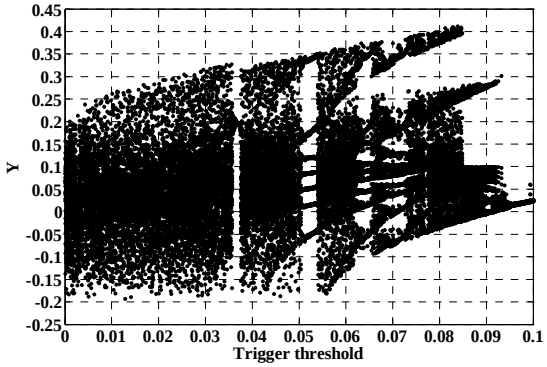

Fig. 3 – Bifurcation diagram at the variation of the threshold, Th.

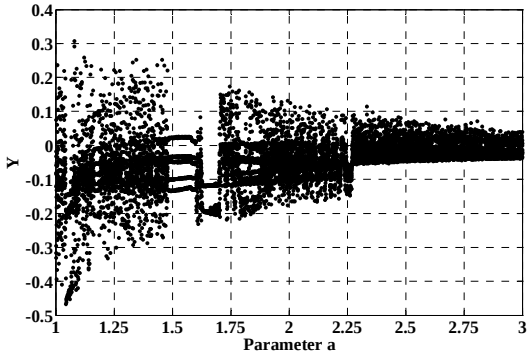

Fig. 4 – Bifurcation diagram at the variation of the parameter *a*.

The ergodic character of the proposed system can be estimated by graphically representing the tridimensional projections of the state portrait, simulated for the equations coefficients, for which the bifurcation diagrams suggested dense clustering of the system attractor. The dense accumulation of the system trajectory, estimates that its closure fills a state space closed sub-domain. Thorough simulations were performed, confirming the ergodic hypothesis, two examples of such results being depicted in Fig. 5. It can be noticed that, for Th = 0.03 and $a = 2.21$, two distinct single scroll strange attractors are obtained, as presented in Fig. 5. Each of these attractors can be attained for different initial conditions. For larger initial values of the state variables *x*, *y* and *z*, the upper attractor, depicted in dotted line in Fig. 5, is attained, whereas negative initial conditions lead to the lower attractor, depicted in continuous line in the same figure. Furthermore, by decreasing coefficient *a* below 1.3, a double scroll attractor is obtained, as presented in Fig. 6, obtained for $a = 1.1$. These simulation results highlight the dynamic richness of the proposed system suggesting the possibility of various types of noise generation.

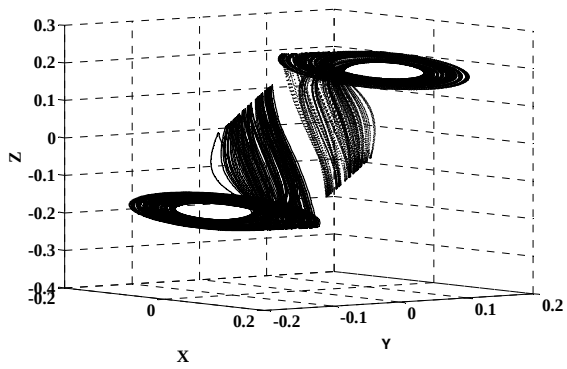

Fig. 5 – 3D projections of the chaotic attractors for $a = 2.21$.

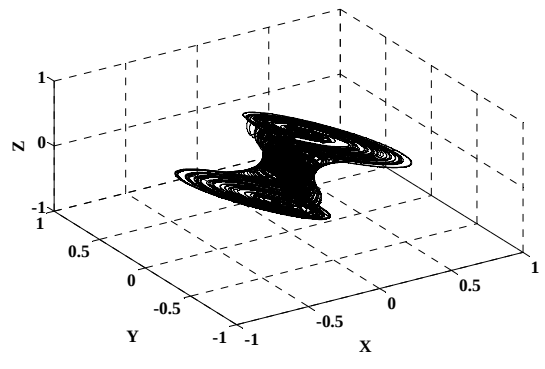

Fig. 6 – 3D projections of the chaotic attractor for $a = 1$.

The sensitivity to initial conditions property of the nonlinear system was verified by simulating two identical systems, for the choice of parameters leading to chaotic dynamics, as suggested by the bifurcation diagrams. The initial conditions of the two systems differ with 10^{-6}. Under these conditions, the RMS value

of the difference between the two state vectors was calculated and depicted in Fig. 7. The fast increase of the RMS error confirms the sensitivity and thus chaotic behavior of the proposed system.

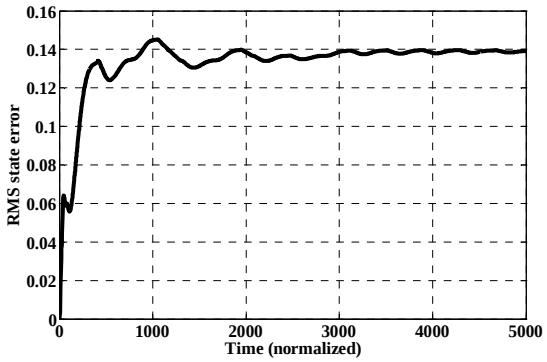

Fig. 7 – RMS value of the difference of the two state vectors.

3. CIRCUIT IMPLEMENTATION

Based on the state equations (4), we designed a circuit implementation of the proposed system. The normalized state equations (4) were de-normalized with the integrators time constant $T = R_1 \cdot C$, leading to the state equations:

$$\begin{cases} T \cdot \mathrm{d}x/\mathrm{d}t = a \cdot y - z \\ T \cdot \mathrm{d}y/\mathrm{d}t = -a \cdot x + z \\ T \cdot \mathrm{d}z/\mathrm{d}t = -x - y - a \cdot z + b \cdot \mathrm{sat}(v) \\ T \cdot \mathrm{d}v/\mathrm{d}t = -G/\tau \cdot (-x) - v/\tau + \mathrm{Th} \cdot G/\tau \cdot \mathrm{sat}(v) \end{cases} \quad (11)$$

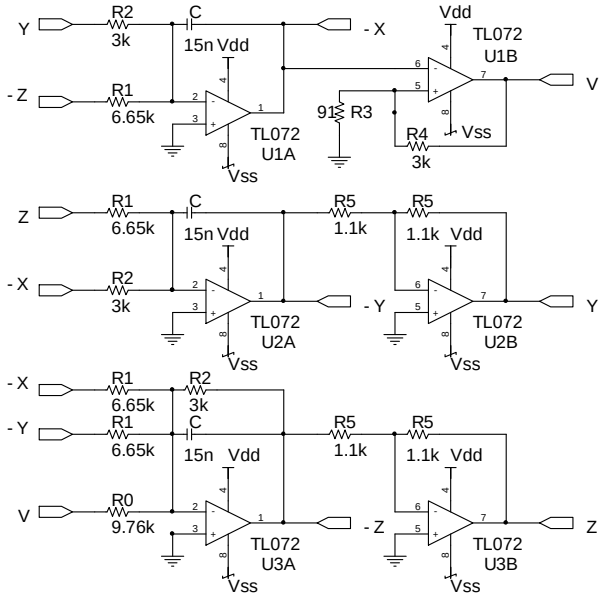

Fig. 8 – The circuit diagram of the implemented circuit.

In equation (11), the sub-unitary de-normalization coefficient *b* aims at scaling the Schmitt trigger output in accordance with the other signal levels to avoid saturation in the other circuit stages.

The resulting circuit, presented in Fig. 8, comprises three OA integrators, implemented with the OA's U1A, U2A and U3A, for the state variables *x*, *y* and *z*, and a Schmitt trigger, implemented with the OA U1B,

for the *v* state variable. Two extra inverters, U2B and U3B, were needed to change the signs of the *y* and *z* state variables. We used three dual OA's, TL072, with $C = 15$ nF capacitors and reference resistors $R_1 = 6.65$ KΩ. All other resistor values are referenced to the R_1 ones, to implement the equations (11) coefficients, $R_2 = R_1 / a$ and $R_0 = R_1 / b$. For the resistor values presented in Fig. 7, the system coefficients are: $a = 2.22$ and $b = 0.68$. The symmetrical thresholds of the Schmitt trigger were imposed by choosing the R_3 and R_4 resistors, leading to a threshold voltage value $V_{Th} = 0.03 \cdot V_{dd}$. The symmetrical supply voltage, $V_{dd} = -V_{ss}$, could be varied between 7 V and 12 V, without structural degradation of the circuit dynamics.

Measurements on the circuit were performed with the Tektronix TDS2002B oscilloscope, digital results being saved and graphically represented on computer. The non-periodic character of the state variables was seen on all time measurements, as in the example in Fig. 9. The measured wideband frequency spectra of the state variables, similar to the example in Fig. 10, were in good accordance to the simulation results. Both simulation and measurement results highlight possible application of the proposed circuit as a random noise generator, useful in situations when low frequency, wideband perturbation signals are needed. A 2D projection of the two-scroll attractor is shown in the example depicted in Fig. 11, where the state variable $y(t)$ was connected to the channel 1 of the oscilloscope and $z(t)$ to the channel 2.

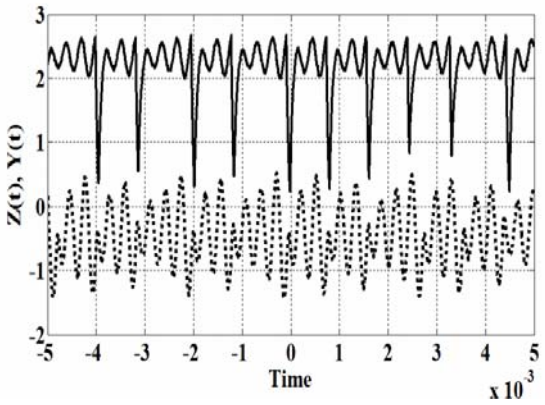

Fig. 9 – Time evolution of the state variables $z(t)$ (continuous line) and $y(t)$ (dotted line).

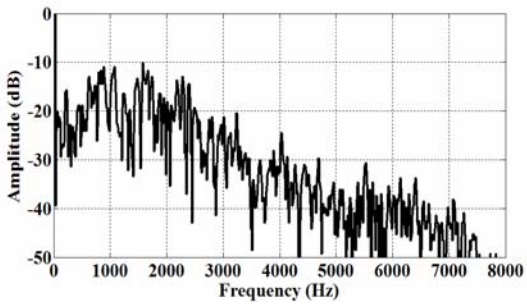

Figure 10 – Frequency spectrum of the *z* state variable.

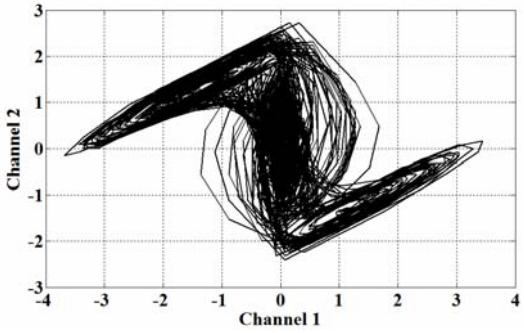

Figure 11 – Projection on the *y* – *z* plane of the double scroll attractor.

Another possible application of the proposed circuit is random pulse generation. If randomly positioned short, sampling pulses are needed, the output of the Schmitt trigger is the most obvious choice, as suggested in the measurements results presented in Fig. 12. The width of the rectangular pulses was measured and showed small variations around the nominal value, $\Delta t = 50$ +/- 10 μs and the period of the sampling pulses varies randomly, leading to a wide frequency spectrum of the form depicted in Fig. 13. By using a comparator for shaping the system state variables to a rectangular form, we can obtain wider pulses with random fronts, as the ones presented in Fig. 14 in the time domain and in Fig. 15 in the frequency one. Such signals may be useful as spread-spectrum clock generators, which are used to reduce the amplitude of EMC perturbations from high current digital systems, at the expense of their wider bandwidth.

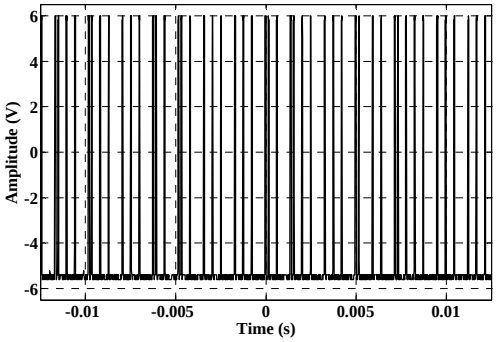

Fig. 12 – Schmitt trigger output pulses waveform.

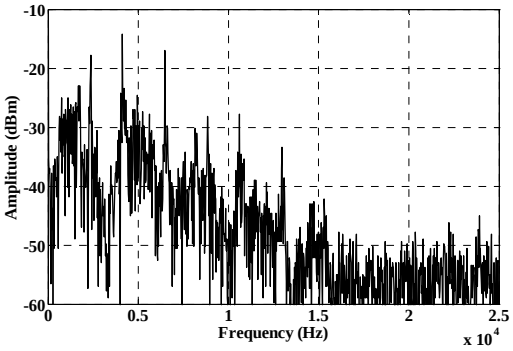

Fig. 13 – Schmitt trigger output spectrum.

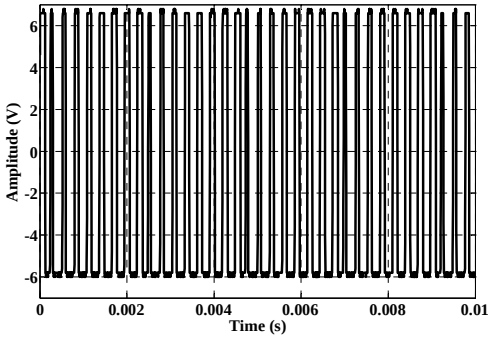

Fig. 14 – Rectangular pulses obtained from the *y* state variable.

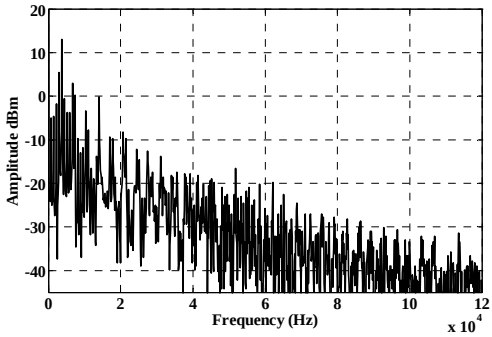

Fig. 15 – Frequency spectrum of the rectangular pulses.

4. CONCLUSION

We introduced a novel, fourth order analog system, using a Schmitt trigger type hysteretic element as nonlinearity. The dynamic behavior of the proposed system was demonstrated analytically and estimated by computer simulations, highlighting its sensitive to initial conditions, ergodic and dissipative nature. Measurements made on the circuit implementation of the proposed system were in good accordance with the theoretical and simulation results. The developed chaos generator is simpler to implement than other circuits reported in the literature, leading to a uniform, repeatable block structure, advantageous for circuit layout. Despite its simplicity, the proposed circuit yields far more complex nonlinear dynamics than all previous implementations, including two chaotic attractors, attainable from different initial conditions, for a wide range of coefficient values, a two scroll chaotic attractor, for a different range of coefficient values, and limit cycles, with different period multiplicity, for smaller ranges of coefficient values. The obtained dynamical richness suggests useful applications in the fields of noise, spread spectrum clock, or random pulses generation.

APPENDIX A

Deducing the state equation of the hysteretic nonlinearity in the proposed system is based on the circuit diagram containing the OA denoted U1B in Fig. 8. We modeled the OA as a differential finite gain, *G*, voltage controlled voltage source. In order to take into account the frequency dependence of the amplifier gain, we included in the model a first order transfer function, containing its dominant pole:

$$H(s)=\frac{1}{\tau s+1}=\frac{1/\tau s}{1+1/\tau s}\cdot \tag{A1}$$

In equation (A1), τ denotes the time constant of the AO, associated with the pole frequency, $\omega_p = 1/\tau$. Denoting by v the OA state variable, by e its input signal and by w its output, the state equation of the amplifier is:

$$v' = -1/\tau \cdot v + G/\tau \cdot e \cdot \tag{A2}$$

Due to the fact that the OA is comprised in a positive, resistive feedback loop, thus working in a nonlinear regime, the saturation characteristic of the OA output stage is modeled as a unit gain, saturation type nonlinearity, sat(·), with normalized breakpoints in the input-output characteristic, as detailed in (3). Thus, the resulting output equation of the Schmitt trigger is:

$$w = \text{sat}(v) \cdot \tag{A3}$$

The differential input stage of the OA receives on its noninverting input the feedback voltage:

$$V_{fb+} = \text{Th} \cdot w \cdot \tag{A4}$$

and the input signal, u, on its inverting one, leading to the formula of the e signal:

$$e = \text{Th} \cdot w - u \cdot \tag{A5}$$

In (A4) and (A5), $\text{Th} = R_3 / R_4$, denotes the Schmitt trigger threshold scaling factor, implemented with the positive feedback resistors, around the U1B OA, in Fig. 8.

Taking into account equations (A2), (A3) and (A5), the state equations of the Schmitt trigger type hysteretic nonlinearity, (A6), is identical with the one used in the system state equations deduction, (2):

$$\begin{cases} \text{d}v/\text{d}t = -\dfrac{v}{\tau} + \text{Th} \cdot \dfrac{G}{\tau} \cdot \text{sat}(v) - \dfrac{G}{\tau} \cdot u; \quad w = \text{sat}(v). \end{cases} \tag{A6}$$

REFERENCES

1. O.E. ROSSLER, *An equation for continuous chaos,* Physics Letters A, **57**, *5*, pp. 397–398, 1976.
2. E.N. LORENZ, *Deterministic nonperiodic flow*, Journal of the Atmospheric Science, **20**, *3*, pp. 130–141, 1963.
3. T. UETA, G. CHEN, *Bifurcation and chaos in Chen's equation*, in Proc. of the IEEE International Symposium on Circuits and Systems, ISCAS 2000, Geneva, Switzerland, **V**, pp. 505–508, 2000, DOI:10.1109/ISCAS.2000.857482
4. C. GRIGORAS, V. GRIGORAS, *Implementation non-ideality influence on the nonlinear dynamics of chaotic generators*, Buletinul Institutului Politehnic din Iasi, Sectia Automatica si calculatoare, **LX (LXIV)**, *1*, pp. 27–36, 2014.
5. C. LI, J.C. SPROTT, W. THIO, H. ZHU, *A unique signum switch for chaos and hyperchaos*, Proc. 7th International Conference on Physics and Control (PhysCon 2015), Istambul, Turkey, 2015.
6. L.O. CHUA, G.-N. LIN, *Canonical realization of Chua's circuit family*, IEEE Transactions on Circuits and Systems, **37**, 7, pp. 885–902, 1990, DOI:10.1109/31.55064.
7. T. TSUBONE, K. HOSHINO, T. SAITO, *Bifurcation from a 3-D hysteresis piecewise-constant circuit*, Proc. of the International Symposium on Circuits and Systems (ISCAS 2001), **3**, Sydney, Australia, pp. 815–818, 2001, DOI:10.1109/ ISCAS.2001.921457
8. T. TSUBONE, T. SAITO, *On basic piecewise-constant systems*, Proc. International Symposium on Circuits and Systems (ISCAS 2000), **1**, Geneva, Switzerland, May, pp. 248–251, 2000, DOI:10.1109/ISCAS.2000.857074
9. J.C. SPROTT, *A new class of chaotic circuit,* Physics Letters A, **266**, *1*, pp. 19–23, 2000, DOI:10.1016/S0375-9601(00)00026-8
10. J.R. PIPER, J.C. SPROTT, *Simple autonomous chaotic circuits*, IEEE Transactions on Circuits and Systems II: Express Briefs, **57**, *9*, pp. 730–734, 2010, DOI:10.1109/TCSII.2010.2058493
11. TEODORESCU H.-N., COJOCARU V., *Complex signal generators based on capacitors and on piezoelectric loads*, Chaos Theory: Modeling, Simulation and Applications, World Scientific Publishing Co., 2011, pp. 423–430.
12. V. GRIGORAS, C. GRIGORAS, *Chaos Based Spread Spectrum Clock Generator*, WSEAS Transactions on Circuits and Systems, **4**, *9*, pp. 1104–1111, 2005.
13. V. GRIGORAS, C. GRIGORAS, *Dynamic and statistic analysis of a simple chaotic generator*, in Proc. the International Symposium on Signals, Circuits and Systems, ISSCS2015, Iasi, Romania, **1**, pp. 122–125, 2015, DOI:10.1109/ISSCS. 2015.7204024.

Received May 11, 2016